

# Performance Analysis of Dual-Hop Mixed PLC/RF Communication Systems

Liang Yang, Xiaoqin Yan, Sai Li, Daniel Benevides da Costa, and Mohamed-Slim Alouini

**Abstract**—In this paper, we study a dual-hop mixed power line communication and radio-frequency communication (PLC/RF) system, where the connection between the PLC link and the RF link is made by a decode-and-forward (DF) or amplify-and-forward (AF) relay. Assume that the PLC channel is affected by both additive background noise and impulsive noise suffers from Log-normal fading, while the RF link undergoes Rician fading. Based on this model, analytical expressions of the outage probability (OP), average bit error rate (BER), and the average channel capacity (ACC) are derived. Furthermore, an asymptotic analysis for the OP and average BER, as well as an upper bound expression for the ACC are presented. At last, numerical results are developed to validate our analytical results, and in-depth discussions are conducted.

**Index Terms**—Average bit error rate (BER), outage probability (OP), average channel capacity (ACC), power line communication, radio-frequency system.

## I. INTRODUCTION

AS a low-cost and energy-saving communication technology, power line communication (PLC) utilizes the existing cables for data transmission [1]- [3]. According to different voltage levels, PLC can communicate through low-voltage cables, medium-voltage cables, and high-voltage cables [4]- [5]. Compared with other methods of communication, PLC has the characteristics of wide coverage, convenient connection, and no need to rewire, which enables it to be used in indoor and outdoor communication. For instance, in [6], the authors put forward a kind of indoor narrow-band PLC network model, and provided the appropriate types of cables and electrical appliances through laboratory experiments and simulation results. Based on the deep integration of PLC and visible light (VLC), a original, practical, and economical indoor broadband broadcasting network was studied in [7]. The authors in [8] investigated the spatial correlation in indoor multiple-input multiple-output (MIMO) PLC channels. Additionally, PLC has arisen as one of the main technical methods of two-way communication in smart grid (SG) [9]. It can be connected to all locations of the grid and transmit data on the original infrastructure. In [10], the authors studied the performance of discrete wavelet multitone transceiver for narrow-band PLC in SG.

However, compared with general wireless communication systems, the performance of PLC communication systems is highly influenced by frequency selectivity, path loss, and various attenuation and interference. In addition, impedance mismatch and non-Gaussian noise in the PLC channel arise as further issues to be tackled with. Moreover, since PLC was originally used to transmit electric energy (and not for

data communication), the transmission power in PLC systems should comply with the regulations of relevant government departments, which leads to the limitation of system capacity and transmission distance [11]. Finally, the affection of background noise (BGN) and impulsive noise (IMN) on system performance should also be jointly considered in PLC systems as they are the main reasons for data loss [12]. In order to alleviate these inconveniences, researchers in the field of PLC have proposed to combine PLC with wireless communication technologies, such as multi-antenna schemes, cooperative communications, MAC protocols, and relaying methods [13]- [15].

Along the years, relay technology has shown to improve the reliability and coverage of the system. Relying on this fact, relay-aided PLC systems have been widely investigated. In [16], a PLC system with Log-normal (LN) fading and Bernoulli-Gaussian IMN assisted by amplify-and-forward (AF) relay was studied, which was shown to outperform PLC systems without embedded relay. The outage probability (OP), average bit error rate (BER), and average channel capacity (ACC) of a mixed decode-and-forward (DF) relay-aided PLC system were derived in [17], while a full-duplex AF relay for PLC networks was considered in [18]. Moreover, the performance of half-duplex PLC networks with either AF or DF relays was examined in [19]. With the aim to enhance the energy efficiency of relaying PLC systems, AF relaying with energy-harvesting capabilities was embedded in a PLC system and accurate expressions for energy efficiency of such systems were derived in [20]. In [21], the authors studied the physical layer security of the relay-aided PLC system with eavesdropping and noise interference. More recently, the authors considered a PLC system with incremental AF and DF relaying, and the results showed a great spectral efficiency improvement [22].

In the aforementioned works dealing with relay-aided PLC systems, the RF links were assumed to undergo LN or Rayleigh fading, although Rician fading arises as a more suitable model owing to the presence of the line-of-sight (LoS) component. As far as the authors know, the performance of PLC/RF systems with both BGN and IMN, where the respective links are modeled by a LN and a Rician distribution, respectively, has not been investigated in the field of PLC. Thus, this paper presents and studies a dual-hop mixed PLC/RF system, assuming both DF and AF relaying protocols.

The original contributions of this paper can be stated as follows:

- A cost-effective and efficient PLC/RF system is introduced and analyzed. The RF system and the PLC system

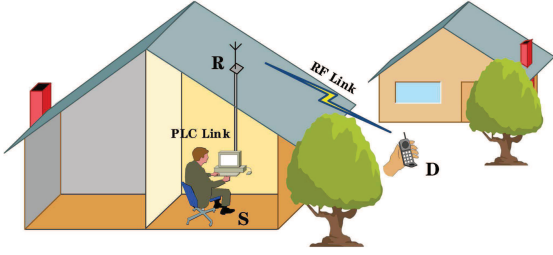


Fig. 1. System setup.

are connected by both DF and AF relaying protocols. The channel of the PLC link is modeled by LN fading and it is subject to additive BGN and IMN, while the RF channel follows a Rician fading distribution.

- For DF relaying, respective expressions for the OP, average BER, and ACC are derived. To get further insights, asymptotic analyses for the OP and average BER are carried out. Moreover, we also derive the upper bound expression for ACC.
- Novel closed-form expressions for the cumulative distribution function (CDF) and probability density function (PDF) of the end-to-end signal-to-noise (SNR) of the considered system with an AF relay are obtained. Moreover, the respective expressions for OP, average BER, as well as ACC are achieved.
- The influences of critical system parameters on the overall performance is studied and insightful discussions are drawn.
- The Monte Carlo simulation results validate our analytical results.

The remaining section of this paper is arranged as follows. Section II introduces the system and channel models. In Section III, a comprehensive performance of the considered system is analyzed, including OP, average BER, and ACC. Section IV provides illustrative numerical examples along with insightful discussions. Finally, Section V concludes the paper. Appendix A provides a detailed proof for the CDF and PDF of the end-to-end SNR.

## II. SYSTEM AND CHANNEL MODELS

Consider a dual-hop mixed PLC/RF communication system, which includes a source node (S), a relay node (R) and a destination node (D), as shown in Fig. 1. In the first time-slot  $T_1$ , the source S transmits data to R through the PLC link modeled by a LN fading distribution with BGN and IMN. Then, during the second time-slot  $T_2$ , by employing DF or AF relaying protocols at R, the signals are sent to D over an RF link modeled by Rician fading. Suppose that direct connection between S and D does not exist.

### A. The PLC Link

By utilizing a binary modulation scheme, the symbol  $x$  from S is transmitted to R through the power cables. Thus, the signal at R can be presented as

$$y_{\text{SR}} = h_{\text{SR}}x + n_{\text{SR}}, \quad (1)$$

where  $n_{\text{SR}}$  represents the additive noise of the PLC channel and  $h_{\text{SR}}$  denotes the channel fading factor. From [23],  $h_{\text{SR}}$  is modeled by a LN distribution and its PDF can be expressed as

$$f_{h_{\text{SR}}}(h_{\text{SR}}) = \frac{1}{h_{\text{SR}}\sqrt{2\pi\sigma_{\text{SR}}^2}} \exp\left(-\frac{(\ln(h_{\text{SR}}) - \mu_{\text{SR}})^2}{2\sigma_{\text{SR}}^2}\right), \quad (2)$$

where  $\sigma_{\text{SR}}^2$  and  $\mu_{\text{SR}}$  denote the variance and mean of  $\ln(h_{\text{SR}})$ , respectively. Due to the random transient switching of low-power components and electrical equipment connected to cables in PLC systems, the interference of both BGN and IMN are considered. In this case, Poisson–Gaussian mixture statistical [23] is employed to model the noise. Thus, the noise in the PLC link can be represented as  $n_{\text{SR}} = n_b + n_i n_p$ , where  $n_b$  is the BGN modeled as the additive white Gaussian noise (AWGN) with zero mean and variance  $\sigma_b^2$ ,  $n_i n_p$  denotes the IMN occurring during  $T$ , with  $n_p$  being defined as the occurrence of the IMN with a rate of  $\lambda$  units per second in the system, which is modeled by a Poisson process, and  $n_i$  represents the AWGN with mean zero and variance  $\sigma_i^2$ . Assuming only the real part of the noise  $n_{\text{SR}}$ , its PDF can be written as [23]

$$f_{n_{\text{SR}}}(n_{\text{SR}}) = \frac{1-P_i}{\sqrt{2\pi\sigma_b^2}} \exp\left(-\frac{n_{\text{SR}}^2}{2\sigma_b^2}\right) + \frac{P_i}{\sqrt{2\pi\sigma_b^2(1+\eta)}} \times \exp\left(-\frac{n_{\text{SR}}^2}{2\sigma_b^2(1+\eta)}\right), \quad (3)$$

where  $P_i = \lambda T$  represents the probability of the occurrence of impulsive noise, and  $\eta = \sigma_i^2/\sigma_b^2$  denotes the ratio of the powers of IMN to BGN.

When there are only BGN samples in the PLC channel, the resulting SNR of the PLC link can be written as

$$\gamma_{\text{SR1}} = \frac{E_b |h_{\text{SR}}|^2}{\sigma_b^2} = \bar{\gamma}_{\text{SR1}} |h_{\text{SR}}|^2, \quad (4)$$

where  $\bar{\gamma}_{\text{SR1}}$  denotes the average SNR of the first hop when only BGN samples are presented and  $E_b$  represents the average energy of the signal. Similarly, when the IMN samples and BGN samples appear simultaneously in the PLC link, the instantaneous SNR can be written as

$$\gamma_{\text{SR2}} = \frac{E_b |h_{\text{SR}}|^2}{\sigma_b^2(1+\eta)} = \bar{\gamma}_{\text{SR2}} |h_{\text{SR}}|^2, \quad (5)$$

where  $\bar{\gamma}_{\text{SR2}}$  is the average SNR of the PLC link when IMN samples and BGN samples occur simultaneously in the system. According to [23], the PDF of the SNR  $\gamma_{\text{SR}}$  of the PLC link can be shown to be given by

$$f_{\gamma_{\text{SR}}}(\gamma) = (1-P_i) \left(\frac{m_1}{\Omega_1}\right)^{m_1} \frac{\gamma^{m_1-1}}{\Gamma(m_1)} \exp\left(-\frac{m_1}{\Omega_1}\gamma\right) + P_i \left(\frac{m_2}{\Omega_2}\right)^{m_2} \frac{\gamma^{m_2-1}}{\Gamma(m_2)} \exp\left(-\frac{m_2}{\Omega_2}\gamma\right), \quad (6)$$

where  $m_1$  and  $m_2$  are defined as the shadowing severity parameters of the Gamma PDF,  $\Omega_1$  and  $\Omega_2$  represent the shadowing area mean power of the Gamma PDF, and  $\Gamma(\cdot)$

is the Gamma function [24]. Thus, the CDF of  $\gamma_{SR}$  can be represented as [23]

$$F_{\gamma_{SR}}(\gamma) = \frac{1-P_i}{\Gamma(m_1)} G_{1,2}^{1,1} \left[ \frac{m_1 \gamma}{\Omega_1} \middle| \begin{matrix} 1 \\ m_1, 0 \end{matrix} \right] + \frac{P_i}{\Gamma(m_2)} G_{1,2}^{1,1} \left[ \frac{m_2 \gamma}{\Omega_2} \middle| \begin{matrix} 1 \\ m_2, 0 \end{matrix} \right], \quad (7)$$

where  $G_{c,d}^{m,n}[\cdot]$  is the Meijer  $G$ -function [24].

### B. The RF Link

In  $T_2$ , R uses DF or AF relaying protocols to forward the received signals to D via the RF channel. It is worthy to say that the RF link between R and D is considered to follow a Rician fading distribution.

1) *DF Case*: For the DF case, we can write the received signal at D as

$$y_{RD}^{DF} = \sqrt{P_R} h_{RD} \hat{x} + n_{RD}, \quad (8)$$

where  $P_R$  denotes the average transmit power at D,  $\hat{x}$  is defined as the signal transmitted from R,  $n_{RD}$  represents the AWGN term with zero mean and variance  $N$ , and  $h_{RD}$  denotes the RF channel coefficient. From (8), the resulting SNR of the RF link can be formulated as

$$\gamma_{RD} = \frac{P_R |h_{RD}|^2}{N} = \bar{\gamma}_{RD} |h_{RD}|^2, \quad (9)$$

where  $\bar{\gamma}_{RD}$  is the average SNR of the RF link. The PDF and CDF of  $\gamma_{RD}$  are given by [25]

$$f_{\gamma_{RD}}(\gamma) = \frac{K+1}{\bar{\gamma}_{RD}} \exp\left(-\frac{(K+1)\gamma_{RD}}{\bar{\gamma}_{RD}} - K\right) \times I_0\left(2\sqrt{K(K+1)\frac{\gamma_{RD}}{\bar{\gamma}_{RD}}}\right), \quad (10)$$

and

$$F_{\gamma_{RD}}(\gamma) = 1 - Q_1\left(\sqrt{2K}, \sqrt{\frac{2(K+1)}{\bar{\gamma}_{RD}}\gamma}\right), \quad (11)$$

where  $I_0(\cdot)$  is the zeroth-order modified Bessel function of the first kind [24],  $K$  ( $K \geq 0$ ) represents the Rician factor, and  $Q_1(\cdot, \cdot)$  is the Marcum Q-function of the first order [26].

2) *AF Case*: For the AF case, the received signal at D is

$$y_{RD}^{AF} = \sqrt{P_R} G h_{RD} y_{SR} + n_{RD}, \quad (12)$$

where  $G$  is the fixed amplifying gain. Thus, the overall instantaneous SNR can be expressed as

$$\gamma_o = \frac{\gamma_{SR} \gamma_{RD}}{C + \gamma_{RD}}, \quad (13)$$

where  $C$  is a constant determined by the AF relay gain  $G$ .

To derive the expression of the PDF of the overall instantaneous SNR  $\gamma_o$  and facilitate our calculation, the approximation of  $I_\nu(x) \simeq \sum_{l=0}^k \frac{\Gamma(k+l)}{\Gamma(l+1)\Gamma(k-l+1)} \frac{k^{1-2l}}{\Gamma(v+l+1)} \left(\frac{x}{2}\right)^{v+2l}$  [26] is used in (10) for  $0 < x < 2k$ . Thus (10) and (11) can be rewritten as

$$f_{\gamma_{RD}}(\gamma) \simeq \frac{K+1}{\bar{\gamma}_{RD}} \exp\left(-\frac{(K+1)\gamma_{RD}}{\bar{\gamma}_{RD}} - K\right) \times \sum_{l=0}^k \frac{\Gamma(k+l) k^{1-2l} K^l (K+1)^l}{\Gamma^2(l+1)\Gamma(k-l+1)\bar{\gamma}_{RD}^l} \gamma^l, \quad (14)$$

and

$$F_{\gamma_{RD}}(\gamma) \simeq 1 - \exp\left(-\frac{(K+1)\gamma_{RD}}{\bar{\gamma}_{RD}} - K\right) \times \sum_{l=0}^k \sum_{r=0}^l \frac{k^{1-2l} K^l (K+1)^r \Gamma(l+k)}{\Gamma(r+1)\Gamma^2(l+1)\Gamma(k-l+1)\bar{\gamma}_{RD}^r} \gamma^r. \quad (15)$$

Then, using the similar method [27], the PDF and CDF of  $\gamma_o$  are derived in (16) and (17) when  $m_1$  and  $m_2$  are integers, shown at the bottom of this page, where  $B_l = \frac{k^{1-2l} K^l \Gamma(k+l)}{\Gamma(k-l+1)\Gamma^2(l+1)}$ .

*Proof*: See Appendix A.

## III. PERFORMANCE ANALYSIS

### A. DF Relaying

1) *OP*: The OP can be defined as the probability that the overall instantaneous SNR is lower than a certain SNR threshold  $\gamma_{th}$ . Thus, by relying on (7) and (11), and making the appropriate substitutions, the outage probability can be determined from the expression below

$$P_{out}^{DF} = \Pr(\min(\gamma_{SR}, \gamma_{RD}) < \gamma_{th}) = F_{\gamma_{SR}}(\gamma_{th}) + F_{\gamma_{RD}}(\gamma_{th}) - F_{\gamma_{SR}}(\gamma_{th}) F_{\gamma_{RD}}(\gamma_{th}). \quad (18)$$

---


$$f_{\gamma_o}(\gamma) = \frac{P_i m_2 \exp(-\frac{m_2 \gamma}{\Omega_2})}{\Omega_2 \Gamma(m_2) \exp(K)} \sum_{l=0}^k \sum_{r=0}^{m_2} \binom{m_2}{r} \left(\frac{m_2 \gamma}{\Omega_2}\right)^{l+m_2-r} \frac{k^{1-2l} K^l (C(K+1))^{l+1} \Gamma(k+l)}{\bar{\gamma}_{RD}^{l+1} \Gamma(k-l+1) \Gamma^2(l+1)} G_{0,2}^{2,0} \left[ \frac{C m_2 (1+K) \gamma}{\Omega_2 \bar{\gamma}_{RD}} \middle| \begin{matrix} - \\ r-l-1, 0 \end{matrix} \right] + \frac{(1-P_i) m_1 \exp(-\frac{m_1 \gamma}{\Omega_1})}{\Omega_1 \Gamma(m_1) \exp(K)} \sum_{l=0}^k \sum_{r=0}^{m_1} \binom{m_1}{r} \left(\frac{m_1 \gamma}{\Omega_1}\right)^{l+m_1-r} \frac{k^{1-2l} K^l (C(K+1))^{l+1} \Gamma(k+l)}{\bar{\gamma}_{RD}^{l+1} \Gamma(k-l+1) \Gamma^2(l+1)} G_{0,2}^{2,0} \left[ \frac{C m_1 (1+K) \gamma}{\Omega_1 \bar{\gamma}_{RD}} \middle| \begin{matrix} - \\ r-l-1, 0 \end{matrix} \right]. \quad (16)$$


---

$$F_{\gamma_o}(\gamma) = F_{\gamma_{SR}}(\gamma) + \frac{(1-P_i) m_1 \exp(-\frac{m_1 \gamma}{\Omega_1})}{\Omega_1 \Gamma(m_1) \exp(K)} \sum_{l=0}^k \sum_{r=0}^{m_1-1} \binom{m_1-1}{r} \left(\frac{m_1 \gamma}{\Omega_1}\right)^{m_1-r-1} B_l G_{1,3}^{2,1} \left[ \frac{C m_1 (1+K) \gamma}{\Omega_1 \bar{\gamma}_{RD}} \middle| \begin{matrix} 1 \\ 1+r, 1+l, 0 \end{matrix} \right] + \frac{P_i m_2 \exp(-\frac{m_2 \gamma}{\Omega_2})}{\Omega_2 \Gamma(m_2) \exp(K)} \sum_{l=0}^k \sum_{r=0}^{m_2-1} \binom{m_2-1}{r} \left(\frac{m_2 \gamma}{\Omega_2}\right)^{m_2-r-1} B_l G_{1,3}^{2,1} \left[ \frac{C m_2 (1+K) \gamma}{\Omega_2 \bar{\gamma}_{RD}} \middle| \begin{matrix} 1 \\ 1+r, 1+l, 0 \end{matrix} \right]. \quad (17)$$

In order to gain further insights on outage probability with the DF protocol, next we derive an asymptotic outage expression. At high SNR, the last term of (18) can be ignored. Then, making use of the following asymptotic series expansion of the Meijer G-function [28, Eq. (07.34.06.0040.01)]

$$G_{c,d}^{m,n} \left( z \left| \begin{matrix} a_1, \dots, a_c \\ b_1, \dots, b_d \end{matrix} \right. \right) = \sum_{\iota=1}^m \frac{\prod_{j=1, j \neq \iota}^m \Gamma(b_j - b_\iota) \prod_{j=1}^n \Gamma(1 - a_j + b_\iota)}{\prod_{j=n+1}^c \Gamma(a_j - b_\iota) \prod_{j=m+1}^d \Gamma(1 - b_j + b_\iota)} z^{b_\iota} (1 + o(z)), \quad (19)$$

the asymptotic  $F_{\gamma_{SR}}(\gamma)$  can be represented as

$$\frac{F_{\gamma_{SR}}(\gamma)}{\bar{\gamma}_{SR} \rightarrow \infty} \simeq \frac{1 - P_i}{\Gamma(1 + m_1)} \left( \frac{m_1 \gamma}{\Omega_1} \right)^{m_1} + \frac{P_i}{\Gamma(1 + m_2)} \left( \frac{m_2 \gamma}{\Omega_2} \right)^{m_2}. \quad (20)$$

Furthermore, the asymptotic expression for  $F_{\gamma_{RD}}(\gamma)$  can be expressed as [29]

$$\frac{F_{\gamma_{RD}}(\gamma)}{\bar{\gamma}_{RD} \rightarrow \infty} \simeq \frac{(1 + K) \gamma}{\bar{\gamma}_{RD} \exp(K)}. \quad (21)$$

Finally, the asymptotic outage probability is attained from the sum of (20) and (21) by setting  $\gamma = \gamma_{th}$ .

2) *Average BER*: Generally, the average BER of a DF relaying system can be formulated as

$$P_{BER}^{DF} = P_{e1} + P_{e2} - 2P_{e1}P_{e2}, \quad (22)$$

where  $P_{e1}$  and  $P_{e2}$  are the average BER of the first hop and the second hop, respectively. In addition, the average BER for various binary modulations can be written as [30]

$$P_b = \frac{q^p}{2\Gamma(p)} \int_0^\infty \exp(-q\gamma) \gamma^{q-1} F_\gamma(\gamma) d\gamma, \quad (23)$$

where  $p$  and  $q$  are parameters related to modulation schemes. In our analysis, we consider the differential binary phase shift keying (DBPSK) scheme (i.e.,  $p = 1, q = 1$ ). Therefore,  $P_1$  and  $P_2$  can be derived as

$$P_{e1} = \frac{1 - P_i}{2\Gamma(m_1)} G_{2,2}^{1,2} \left[ \frac{m_1}{\Omega_1} \left| \begin{matrix} 0, 1 \\ m_1, 0 \end{matrix} \right. \right] + \frac{P_i}{2\Gamma(m_2)} G_{2,2}^{1,2} \left[ \frac{m_2}{\Omega_2} \left| \begin{matrix} 0, 1 \\ m_2, 0 \end{matrix} \right. \right], \quad (24)$$

$$P_{e2} = \frac{1 + K}{2(1 + K + \bar{\gamma}_{RD}) \exp(K)} {}_1F_1 \left( 1; 1; \frac{K(K+1)}{K+1 + \bar{\gamma}_{RD}} \right), \quad (25)$$

where  ${}_1F_1(\cdot)$  is the confluent hypergeometric function [24]. By substituting (24) and (25) into (22), we obtain the average BER expression. Since the last term in (22) can be negligible at high SNRs, one can obtain the asymptotic average BER as follows

$$P_{BER}^{DF} \rightarrow P_{e1}^A + P_{e2}^A, \quad (26)$$

where  $P_{e1}^A$  and  $P_{e2}^A$  denote the asymptotic BER of  $P_{e1}$  and  $P_{e2}$ , respectively. Substituting (20) into (23), the expression of  $P_{e1}^A$  can be obtained by

$$P_{e1}^A = \frac{1 - P_i}{2} \left( \frac{m_1}{\Omega_1} \right)^{m_1} + \frac{P_i}{2} \left( \frac{m_2}{\Omega_2} \right)^{m_2}. \quad (27)$$

Then, according [29], the  $P_{e2}^A$  can be expressed as

$$P_{e2}^A = \frac{(1 + K) \Gamma(2)}{2\bar{\gamma}_{RD} \exp(K)}. \quad (28)$$

3) *Average Channel Capacity*: Generally, the overall capacity of the dual-hop DF system can be defined as

$$C_{DF} = \frac{1}{2} \mathbb{E} \{ \log_2(1 + \gamma) \} = \frac{1}{2 \ln(2)} \int_0^\infty \ln(1 + \gamma) f_\gamma(\gamma) d\gamma = \frac{1}{2 \ln(2)} (C_1 + C_2 - C_3 - C_4), \quad (29)$$

where  $f_\gamma(\gamma) = f_{\gamma_{SR}}(\gamma) + f_{\gamma_{RD}}(\gamma) - f_{\gamma_{SR}}(\gamma)F_{\gamma_{RD}}(\gamma) - F_{\gamma_{SR}}(\gamma)f_{\gamma_{RD}}(\gamma)$ . By utilizing  $\ln(1 + \gamma) = G_{2,2}^{1,2} \left[ \gamma \left| \begin{matrix} 1, 1 \\ 1, 0 \end{matrix} \right. \right]$  [28, Eq. (01.04.26.0003.01)],  $\exp(-bz) = G_{0,1}^{1,0} [bz | \bar{\cdot}]$  [28, Eq. (07.34.21.0013.01)], [28, Eq. 07.34.21.0088.01] and [28, Eq. 07.34.21.0081.01], expressions for  $C_1$ ,  $C_2$ ,  $C_3$  and  $C_4$  can be calculated as

$$C_1 = \frac{1 - P_i}{\Gamma(m_1)} G_{3,2}^{1,3} \left[ \frac{\Omega_1}{m_1} \left| \begin{matrix} 1 - m_1, 1, 1 \\ 1, 0 \end{matrix} \right. \right] + \frac{P_i}{\Gamma(m_2)} G_{3,2}^{1,3} \left[ \frac{\Omega_2}{m_2} \left| \begin{matrix} 1 - m_2, 1, 1 \\ 1, 0 \end{matrix} \right. \right], \quad (30)$$

$$C_2 = \sum_{l=0}^k \frac{\Gamma(k+l) k^{1-2l} K^l}{\Gamma(k-l+1) \Gamma^2(l+1) \exp(K)} G_{3,2}^{1,3} \left[ \frac{\bar{\gamma}_{RD}}{K+1} \left| \begin{matrix} -l, 1, 1 \\ 1, 0 \end{matrix} \right. \right], \quad (31)$$

$$C_3 = \frac{(P_i - 1) \left( \frac{m_1}{\Omega_1} \right)^{m_1}}{\Gamma(m_1) \exp(K)} \sum_{l=0}^k \sum_{r=0}^l \Gamma(l+1) B_l \Theta_r W_{1r} G_{3,2}^{1,3} [W_{1r} |_{\varsigma_{1r}}^{1,0}] + C_1 - \frac{P_i \left( \frac{m_2}{\Omega_2} \right)^{m_2}}{\Gamma(m_2) \exp(K)} \sum_{l=0}^k \sum_{r=0}^l \Gamma(l+1) B_l \Theta_r W_{2r} G_{3,2}^{1,3} [W_{2r} |_{\varsigma_{2r}}^{1,0}], \quad (32)$$

and

$$C_4 = \frac{1 - P_i}{\Gamma(m_1) \exp(K)} \sum_{l=0}^k B_l \times G_{1,0;2,2;1,2}^{0,1;1,2;1,1} \left[ \begin{matrix} -l \\ - \end{matrix} \left| \begin{matrix} 1, 1 \\ 1, 0 \end{matrix} \right. \frac{1}{m_1, 0} \left| \frac{\bar{\gamma}_{RD}}{K+1}, \frac{\Omega_1 \bar{\gamma}_{RD}}{m_1 (K+1)} \right. \right] + \frac{P_i}{\Gamma(m_2) \exp(K)} \sum_{l=0}^k B_l \times G_{1,0;2,2;1,2}^{0,1;1,2;1,1} \left[ \begin{matrix} -l \\ - \end{matrix} \left| \begin{matrix} 1, 1 \\ 1, 0 \end{matrix} \right. \frac{1}{m_2, 0} \left| \frac{\bar{\gamma}_{RD}}{K+1}, \frac{\Omega_2 \bar{\gamma}_{RD}}{m_2 (K+1)} \right. \right], \quad (33)$$

where  $\varsigma_{1r} = \{1 - m_1 - r, 1, 1\}$ ,  $\varsigma_{2r} = \{1 - m_2 - r, 1, 1\}$ ,  $\Theta_r = \frac{(K+1)^r}{\bar{\gamma}_{RD} \Gamma(r+1)}$ ,  $W_{1r} = \left( \frac{\Omega_1 \bar{\gamma}_{RD}}{m_1 \bar{\gamma}_{RD} + \Omega_1 (K+1)} \right)^{m_1 + r}$ ,  $W_{2r} = \left( \frac{\Omega_2 \bar{\gamma}_{RD}}{m_2 \bar{\gamma}_{RD} + \Omega_2 (K+1)} \right)^{m_2 + r}$ . Furthermore, an upper bound for  $C_{DF}$  can be formulated as [31]

$$C_{DF} = \frac{1}{2} \mathbb{E} \{ \log_2(1 + \gamma) \} \leq \frac{1}{2} \log_2(1 + \mathbb{E}(\gamma)), \quad (34)$$

where the mean value  $\mathbb{E}(\gamma) = \int_0^\infty \gamma f_\gamma(\gamma) d\gamma$  can be calculated as (35), shown at the top of this page.

$$\begin{aligned}
\mathbb{E}(\gamma) &= \frac{(1-P_i) \binom{m_1}{\Omega_1}^{m_1}}{\Gamma(m_1) \exp(K)} \sum_{l=0}^k \sum_{r=0}^l \Gamma(l+1) \Gamma(m_1+r) B_l \Theta_r W_{1r} + \frac{P_i \binom{m_2}{\Omega_2}^{m_2}}{\Gamma(m_2) \exp(K)} \sum_{l=0}^k \sum_{r=0}^l \Gamma(l+1) \Gamma(m_2+r) B_l \Theta_r W_{2r} \\
&\quad - \frac{(1-P_i) \bar{\gamma}_{RD} \exp(-K)}{(K+1) \Gamma(m_1)} \sum_{l=0}^k B_l G_{2,2}^{1,2} \left[ \frac{m_1 \bar{\gamma}_{RD}}{\Omega_1 (K+1)} \middle| \begin{matrix} -l-1, 1 \\ m_1, 0 \end{matrix} \right] - \frac{P_i \bar{\gamma}_{RD} \exp(-K)}{(K+1) \Gamma(m_2)} \sum_{l=0}^k B_l G_{2,2}^{1,2} \left[ \frac{m_2 \bar{\gamma}_{RD}}{\Omega_2 (K+1)} \middle| \begin{matrix} -l-1, 1 \\ m_2, 0 \end{matrix} \right] \\
&\quad + \frac{\bar{\gamma}_{RD}}{(K+1) \exp(K)} \sum_{l=0}^k B_l \Gamma(l+2). \tag{35}
\end{aligned}$$

$$\begin{aligned}
P_{\text{BER}}^{AF} &= \frac{1-P_i}{2\Gamma(m_1)} G_{2,2}^{1,2} \left[ \frac{m_1}{\Omega_1} \middle| \begin{matrix} 0, 1 \\ m_1, 0 \end{matrix} \right] + \frac{P_i}{2\Gamma(m_2)} G_{2,2}^{1,2} \left[ \frac{m_2}{\Omega_2} \middle| \begin{matrix} 0, 1 \\ m_2, 0 \end{matrix} \right] \\
&\quad + \frac{(1-P_i) \Omega_1 \exp(-K)}{2\Gamma(m_1+1)} \sum_{l=0}^k \sum_{r=0}^{m_1-1} \binom{m_1-1}{r} \left( \frac{m_1+\Omega_1}{m_1} \right)^{r-m_1} B_l G_{2,3}^{2,2} \left[ \frac{C m_1 (1+K)}{\bar{\gamma}_{RD} (m_1+\Omega_1)} \middle| \begin{matrix} 1+r-m_1, 1 \\ 1+r, 1+l, 0 \end{matrix} \right] \\
&\quad + \frac{P_i \Omega_2 \exp(-K)}{2\Gamma(m_2+1)} \sum_{l=0}^k \sum_{r=0}^{m_2-1} \binom{m_2-1}{r} \left( \frac{m_2+\Omega_2}{m_2} \right)^{r-m_2} B_l G_{2,3}^{2,2} \left[ \frac{C m_2 (1+K)}{\bar{\gamma}_{RD} (m_2+\Omega_2)} \middle| \begin{matrix} 1+r-m_2, 1 \\ 1+r, 1+l, 0 \end{matrix} \right]. \tag{37}
\end{aligned}$$

$$\begin{aligned}
C_{AF} &= \frac{(1-P_i) \exp(-K)}{2\Gamma(m_1) \ln(2)} \sum_{l=0}^k \sum_{r=0}^{m_1} \binom{m_1}{r} \left( \frac{C(1+K)}{\bar{\gamma}_{RD}} \right)^{l+1} B_l G_{1,0;2,2;0,2}^{0,1;1,2;2,0} \left[ \begin{matrix} r-m_1-l \\ - \end{matrix} \middle| \begin{matrix} 1, 1 \\ 1, 0 \end{matrix} \middle| \begin{matrix} - \\ r-l-1, 0 \end{matrix} \middle| \frac{\Omega_1}{m_1}, \frac{C(1+K)}{\bar{\gamma}_{RD}} \right] \\
&\quad + \frac{P_i \exp(-K)}{2\Gamma(m_2) \ln(2)} \sum_{l=0}^k \sum_{r=0}^{m_2} \binom{m_2}{r} \left( \frac{C(1+K)}{\bar{\gamma}_{RD}} \right)^{l+1} B_l G_{1,0;2,2;0,2}^{0,1;1,2;2,0} \left[ \begin{matrix} r-m_2-l \\ - \end{matrix} \middle| \begin{matrix} 1, 1 \\ 1, 0 \end{matrix} \middle| \begin{matrix} - \\ r-l-1, 0 \end{matrix} \middle| \frac{\Omega_2}{m_2}, \frac{C(1+K)}{\bar{\gamma}_{RD}} \right]. \tag{39}
\end{aligned}$$

## B. Fixed-Gain AF Relaying

1) *OP*: For the AF relaying scheme, OP can be formulated as

$$P_{\text{out}}^{AF} = \Pr \left\{ \frac{\gamma_{SR} \bar{\gamma}_{RD}}{C + \gamma_{RD}} < \gamma_{\text{th}} \right\} = F_{\gamma_o}(\gamma_{\text{th}}), \tag{36}$$

where  $F_{\gamma_o}(\gamma_{\text{th}})$  denotes the CDF of  $\gamma_o$  when  $\gamma = \gamma_{\text{th}}$ .

2) *Average BER*: Assuming DBPSK scheme, the average BER for the considered cooperative PLC/RF system with fixed-gain AF relaying can be expressed as  $P_{\text{BER}}^{AF} = \frac{1}{2} \int_0^\infty \exp(-\gamma) F_{\gamma_o}(\gamma) d\gamma$ . After some algebraic calculations, we can arrive at the average BER in (37), shown at the top of this page.

3) *Average Channel Capacity*: By employing AF protocol, the ACC can be formulated as

$$C_{AF} = \frac{1}{2} \mathbb{E} \{ \log_2(1+\gamma_o) \} = \frac{1}{2 \ln(2)} \int_0^\infty \ln(1+\gamma) f_{\gamma_o}(\gamma) d\gamma. \tag{38}$$

Then, upon substituting (16) in (38) and using the integral from three Meijer  $G$ -functions [28, Eq. 07.34.21.0081.01],  $C_{AF}$  is given by (39), shown at the top of this page.

Furthermore, an upper bound for  $C_{AF}$  can be represented as

$$C_{AF} = \frac{1}{2} \mathbb{E} \{ \log_2(1+\gamma_o) \} \leq \frac{1}{2} \log_2(1 + \mathbb{E}(\gamma_o)), \tag{40}$$

where

$$\begin{aligned}
\mathbb{E}(\gamma_o) &= \frac{(1-P_i) \Omega_1 \exp(-K)}{\Gamma(1+m_1)} \sum_{l=0}^k \sum_{r=0}^{m_1} \binom{m_1}{r} \left( \frac{C(1+K)}{\bar{\gamma}_{RD}} \right)^{l+1} \\
&\quad \times B_l G_{2,1}^{1,2} \left[ \frac{C(1+K)}{\bar{\gamma}_{RD}} \middle| \begin{matrix} r-m_1-l-1 \\ r-l-1, 0 \end{matrix} \right] \\
&\quad + \frac{P_i \Omega_2 \exp(-K)}{\Gamma(1+m_2)} \sum_{l=0}^k \sum_{r=0}^{m_2} \binom{m_2}{r} \left( \frac{C(1+K)}{\bar{\gamma}_{RD}} \right)^{l+1} \\
&\quad \times B_l G_{2,1}^{1,2} \left[ \frac{C(1+K)}{\bar{\gamma}_{RD}} \middle| \begin{matrix} r-m_2-l-1 \\ r-l-1, 0 \end{matrix} \right]. \tag{41}
\end{aligned}$$

## IV. SIMULATION AND NUMERICAL RESULTS

In this section, numerical examples are presented to illustrate the analytical and asymptotic expressions developed in the previous section. Additionally, Monte-Carlo simulation results corroborate the analytical analysis. Unless otherwise specified, we set  $m_1 = m_2 = 8$ ,  $P_i = 0.2$ ,  $\eta = 5$ ,  $\sigma_{SR} = 0.23$ ,  $K = 6$  dB,  $C = 1.2$ ,  $G = 3$ ,  $\gamma_{th} = 0$  dB and  $\bar{\gamma}_{SR} = \bar{\gamma}_{RD} = \bar{\gamma}$ .

In Fig. 2, OP versus  $\bar{\gamma}$  is plotted for various values of  $K$ , and assuming the considered dual-hop mixed PLC/RF system with the DF protocol. In addition, we set  $K = 2, 4, 6$  dB. It can be clearly noted that the system outage performance improves by increasing the values of  $K$ . The reason is that  $K$  is the ratio of the powers of the LoS components to the powers of the scattered components. The higher the values of  $K$ , the lower the signal attenuation caused by multipath effects.

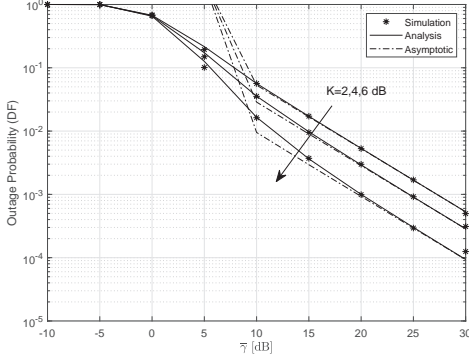


Fig. 2. Outage probability for different values of  $K$  (DF protocol).

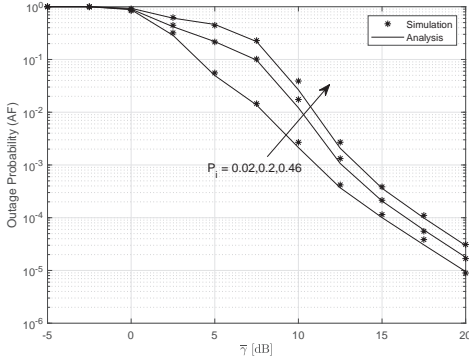


Fig. 3. Outage probability for various values of  $P_i$  (AF protocol).

Furthermore, Fig. 2 shows that the asymptotic  $P_{out}^{DF}$  expression converges to the exact  $P_{out}^{DF}$  expression at high SNRs. In Fig. 3, we draw  $P_{out}^{AF}$  versus  $\bar{\gamma}$  for various values of  $P_i$  assuming the AF protocol. From Fig. 3, it can be observed that for low values of  $P_i$ ,  $P_{out}^{AF}$  is highly degraded, resulting in a better performance. This is because  $P_i$  represents the probability of the arrival of the impulsive noise, and lower values of  $P_i$  generates a weak effect of the IMN for the PLC/RF system. Finally, Fig. 4 presents the outage performance of the dual-hop PLC/RF system with different values of threshold SNR  $C_{th}$  under DF and AF relay protocols. From Fig. 4, it can be noted that the outage performance with the AF relay protocol is superior to the outage performance with the DF relay protocol, and the performance increases when the value  $\gamma_{th}$  decreases.

In Fig. 5, the average BER versus average SNR  $\bar{\gamma}$  is plotted under different values of  $K$ , and considering the DF relay protocol. This figure demonstrates the average BER performance with higher values  $K$  performs much better than the one with the lower values of  $K$ . The reason is because higher values of  $K$  means more LoS components, which improves the system performance. Additionally, Fig. 5 also reveals the convergence between the asymptotic and exact  $P_{BER}^{DF}$  expressions. The impact of the different values of  $P_i$  is shown in Fig. 6. As can be seen, a decrease in the value of  $P_i$  (the probability of impulse noise reaching the PLC channel) leads to a BER decrease, which results in a better system

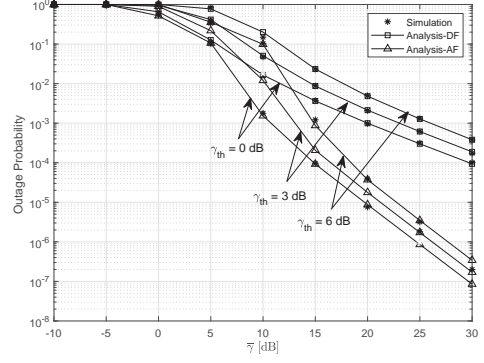


Fig. 4. Outage probability for various values of  $\gamma_{th}$  under different relaying protocols.

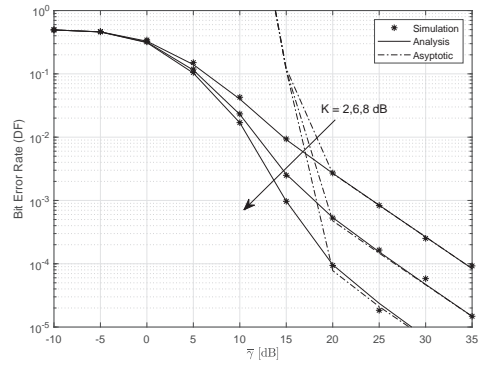


Fig. 5. BER for different Rician factors  $K$  (DF protocol).

performance. The reason is that with the decrease of IMN arriving at the system, the severity of IMN component in the system decreases compared with the BGN sample, improving consequently the performance. In Fig. 7, the average BER is presented under different values of  $\eta$ . It can be clearly seen that a decrease in  $\eta$  leads to a lower average BER. Similar to the results obtained previously to outage probability, it is shown that the average BER of the AF protocol is significantly superior to the BER performance of the DF one.

Fig. 8 plots the ACC  $C_{DF}$  versus  $\bar{\gamma}$  for various values of  $\eta$ . It can be observed that  $C_{DF}$  increases with the decrease of  $\eta$ . In addition, we plot the asymptotic  $C_{DF}$ , which reveals the correctness of the asymptotic expression of  $C_{DF}$ . In Fig. 9, we plot exact average channel capacity  $C_{AF}$  versus  $\bar{\gamma}$  for various values of  $P_i$ . As can be seen, higher  $C_{AF}$  can be obtained when the values of  $P_i$  decrease. Also, it is shown the convergence between the asymptotic and exact  $C_{AF}$  expressions.

## V. CONCLUSIONS

In this work, we studied the performance of the PLC/RF system under both DF and AF relay protocols. It was supposed that the PLC link is modeled by a LN distribution with IMN while the RF link follows the Rician distribution. Closed-form expressions for the OP, average BER, and ACC were derived. For AF relaying, analytical expressions for the CDF and PDF

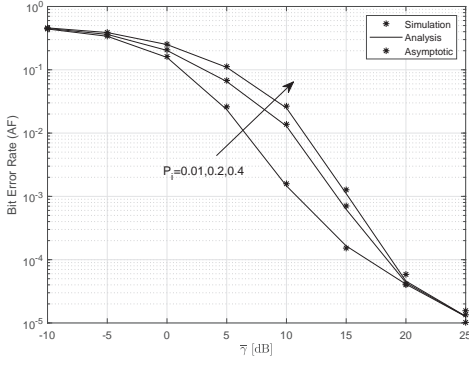


Fig. 6. BER for various values of  $P_i$  (AF protocol).

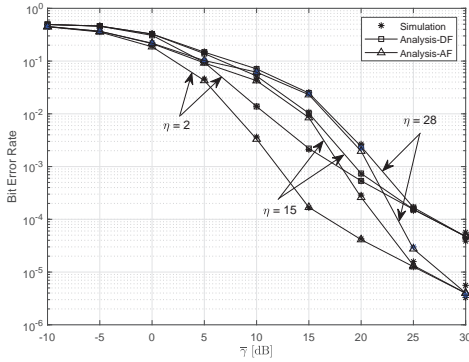


Fig. 7. BER for various values of  $\eta$  under different relaying protocols.

of the end-to-end SNR have been obtained in closed-form. For DF relaying, closed-form expressions for the asymptotic OP, average BER, and ACC were derived. The analytical expressions were validated with their corresponding simulation results. Additionally, it was studied the impact of impulsive noise and Rician factor on the overall system performance, and insightful discussions were drawn.

#### APPENDIX A PDF AND CDF OF THE END-TO-END SNR

In this section, we derive the PDF and CDF of the end-to-end overall SNR  $\gamma_o$ . Similar methods can also be found in [27]. The PDF of  $\gamma_o = \frac{\gamma_{SR}\gamma_{RD}}{C+\gamma_{RD}}$  can be written as

$$\begin{aligned} f_{\gamma_o}(\gamma) &= \frac{d}{d\gamma} \Pr \left\{ \frac{\gamma_{SR}\gamma_{RD}}{C+\gamma_{RD}} < \gamma \right\} \\ &= \frac{d}{d\gamma} \int_0^\infty \Pr \left\{ \frac{\gamma_{RD}x}{C+\gamma_{RD}} < \gamma \right\} f_{\gamma_{SR}}(x) dx \\ &= \frac{d}{d\gamma} \left[ \int_0^\gamma \Pr \{ \gamma_{RD}(x-\gamma) < C\gamma \} f_{\gamma_{SR}}(x) dx \right. \\ &\quad \left. + \int_\gamma^\infty \Pr \{ \gamma_{RD}(x-\gamma) < C\gamma \} f_{\gamma_{SR}}(x) dx \right]. \quad (42) \end{aligned}$$

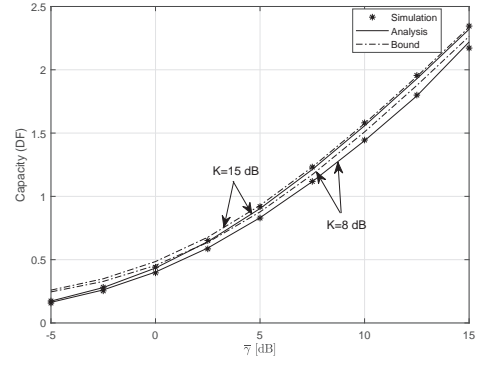


Fig. 8. Ergodic channel capacity for various values of  $K$  (DF protocol).

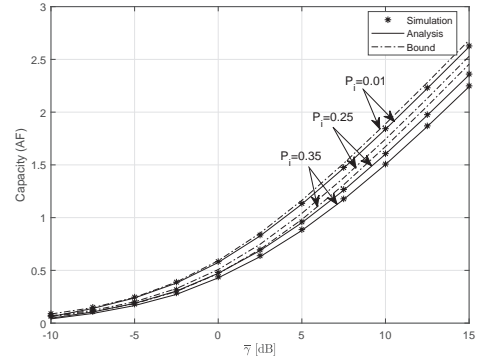


Fig. 9. Ergodic channel capacity for different values of  $P_i$  (AF protocol).

Due to  $0 < x < \gamma$ ,  $\Pr \{ \gamma_{RD}(x-\gamma) < C\gamma \} = 1$ , (42) can be rewritten as

$$\begin{aligned} f_{\gamma_o}(\gamma) &= \frac{d}{d\gamma} \left[ \int_0^\gamma f_{\gamma_{SR}}(x) dx \right. \\ &\quad \left. + \int_\gamma^\infty \Pr \left\{ \gamma_{RD} < \frac{C\gamma}{x-\gamma} \right\} f_{\gamma_{SR}}(x) dx \right] \\ &= f_{\gamma_{SR}}(\gamma) - \lim_{x \rightarrow \gamma^+} \Pr \left\{ \gamma_{RD} < \frac{C\gamma}{x-\gamma} \right\} f_{\gamma_{SR}}(\gamma) \\ &\quad + \int_\gamma^\infty f_{\gamma_{RD}} \left( \frac{C\gamma}{x-\gamma} \right) \frac{cx}{(x-\gamma)^2} f_{\gamma_{SR}}(x) dx. \quad (43) \end{aligned}$$

Since  $\lim_{x \rightarrow \gamma^+} \Pr \left\{ \gamma_{RD} < \frac{C\gamma}{x-\gamma} \right\} = 1$ , one can obtain

$$f_{\gamma_o}(\gamma) = \int_\gamma^\infty f_{\gamma_{RD}} \left( \frac{C\gamma}{x-\gamma} \right) \frac{cx}{(x-\gamma)^2} f_{\gamma_{SR}}(x) dx. \quad (44)$$

By substituting  $t = x-\gamma$  in (44) and applying (6), (14),  $f_{\gamma_o}(\gamma)$  can be formulated as

$$\begin{aligned} f_{\gamma_o}(\gamma) &= \frac{\exp(-\frac{m_1}{\Omega_1}\gamma) \left(\frac{m_1}{\Omega_1}\right)^{m_1}}{\Gamma(m_1) \exp(K)} \sum_{l=0}^k \left( \frac{C(1+K)}{\bar{\gamma}_{RD}} \right)^{l+1} B_l \gamma^l \Phi_1 \\ &\quad + \frac{\exp(-\frac{m_2}{\Omega_2}\gamma) \left(\frac{m_2}{\Omega_2}\right)^{m_2}}{\Gamma(m_2) \exp(K)} \sum_{l=0}^k \left( \frac{C(1+K)}{\bar{\gamma}_{RD}} \right)^{l+1} B_l \gamma^l \Phi_2, \quad (45) \end{aligned}$$

where  $\Phi_\rho$ ,  $\rho = 1, 2$  are expressed as

$$\Phi_\rho = \int_0^\infty \left(1 + \frac{\gamma}{t}\right)^{m_\rho} t^{m_\rho - l - 2} \times \exp\left(-\frac{m_\rho t}{\Omega_\rho}\right) \exp\left(-\frac{C(K+1)}{t\bar{\gamma}_{RD}}\gamma\right) dt. \quad (46)$$

Using  $\exp(-bz) = G_{0,1}^{1,0} [bz | -]$ , the integral formula [28, Eq. (07.34.21.0088.01)] and the expanding expression of  $(1 + \gamma/t)^{m_\rho}$ ,  $\rho = 1, 2$  [27], (16) is obtained.

From (43), the CDF of  $\gamma_o$  can be written as

$$F_{\gamma_o}(\gamma) = F_{\gamma_{SR}}(\gamma) + \int_\gamma^\infty F_{\gamma_{RD}}\left(\frac{C\gamma}{x-\gamma}\right) f_{\gamma_{SR}}(x) dx. \quad (47)$$

To simplify the operation, we use the new expression of  $F_{\gamma_{RD}}(\gamma) = \sum_{l=0}^k \frac{k^{l-2l} K^l \Gamma(k+l)}{\Gamma(k-l+1) \Gamma^2(k+1) \exp(K)} \Upsilon(l+1, \frac{(K+1)\gamma}{\bar{\gamma}_{RD}})$  obtained from the integration of (14) to (47). Therefore, the CDF of  $\gamma_o$  is represented by (17).

## REFERENCES

- [1] Ferreira, H. C., Lampe, L., Newbury, J., Swart, T. G., *Power Line Communications: Theory and Applications for Narrowband and Broadband Communications over Power Lines*, Singapore: Wiley, 2010
- [2] A. Majumder and J. Caffery, Jr., "Power line communications: an overview," *IEEE Potentials*, vol. 23, no. 4, pp. 48, Oct./Nov. 2004
- [3] Y. Qian, C. Zhang, Z. Xu, F. Shu, L. Dong, J. Li, "A reliable opportunistic routing for smart grid with in-home power line communication networks," *Sci. China Inf. Sci.*, Volume 59, Issue 12, 2016, Pages 122305-, ISSN 1674-733X.
- [4] V. V. Kharlamov, S. E. Romanov, Y. P. Shkarin and A. G. Merkulov, "Characteristics of PLC channels over high voltage power cables and mixed cable-overhead high voltage power lines," *IEEE GPECOM, Nevsehir, Turkey*, pp. 35-40, 2019.
- [5] D. B. Unsal, A. H. Koc, T. Yalcinoz and I. Onaran, "Medium voltage and low voltage applications of new power line communication model for smart grids," *ENERGYCON, Leuven*, pp. 1-6, 2016.
- [6] T. A. Papadopoulos, G. C. Argyropoulos, B. D. Sarantinos and G. K. Papagiannis, "Analysis of indoor PLC networks: laboratory tests and simulation results," *IEEE Lausanne Power Tech.*, pp. 1935-1940, 2007.
- [7] H. Ma, L. Lampe and S. Hranilovic, "Integration of indoor visible light and power line communication systems," *IEEE Int. Symp. Power Line Commun.*, pp. 291-296, 2013.
- [8] K. Khalil, M.G. Gazalet, P. Corlay et al., "An MIMO random channel generator for indoor power-line communication", *IEEE Trans. Power Deliv.*, vol. 29, no. 4, pp. 1561-1568, 2014.
- [9] A. Sendin, J. Simon, I. Urrutia and I. Berganza, "PLC deployment and architecture for smart grid applications in Iberdrola", *IEEE ISPLC*, pp. 173-178, 2014.
- [10] S. Baig and J. Yazdani, "Performance analysis of discrete wavelet multitone transceiver for narrowband PLC in smart grid", *IEEE PES Int. Conf. Exhib. Innov. Smart Grid Technol.*, pp. 1-6, Dec. 2011.
- [11] N.A.T.O. Research and T. Organisation, "HF interference, procedures and tools-final report of NATO RTO information systems technology panel research task group IST- 050/RTG-022," Jun. 2007. 12, 34, 39, 41, 128.
- [12] M.K. Simon, M.S. Alouini, *Digital communication over fading channels*, Wiley, New York, 2000.
- [13] A. Schwager, D. Schneider, W. Baschlin, A. Dilly, and J. Speidel, "MIMO PLC: Theory, measurements and system setup," *IEEE Int. Symp. Power Line Commun. and Its Appl. (ISPLC)*, pp. 4853, Apr. 2011.
- [14] L. Lampe and A. Vinck, "Cooperative multihop power line communications," *IEEE Int. Symp. Power Line Commun. and Its Appl. (ISPLC)*, pp. 16, Mar. 2012.
- [15] X. Cheng, R. Cao, and L. Yang, "Relay-aided amplify-and-forward powerline communications," *IEEE Trans. Smart Grid*, vol. 4, pp. 265272, Mar. 2013.
- [16] A. Dubey and R. K. Mallik, "PLC system performance with AF relaying," *IEEE Trans. Commun.*, vol. 63, no. 6, pp. 2337-2345, June 2015.
- [17] A. Dubey, R. K. Mallik and R. Schober, "Performance analysis of a multi-hop power line communication system over log-normal fading in presence of impulsive noise," *IET Commun.*, vol. 9, no. 1, pp. 1-9, 2015.
- [18] F. Passerini and A. M. Tonello, "Analog full-duplex amplify-and-forward relay for power line communication networks," *IEEE Commun. Lett.*, vol. 23, no. 4, pp. 676-679, April 2019.
- [19] R. K. Ahiadormey, P. Anokye, H. Jo and K. Lee, "Performance analysis of two-way relaying in cooperative power line communications," *IEEE Access*, vol. 7, pp. 97264-97280, 2019.
- [20] K. M. Rabie, B. Adebisi and A. Salem, "Improving energy efficiency in dual-hop cooperative PLC relaying systems," *International Symposium on Power Line Communications and its Applications (ISPLC)*, Bottrop, pp. 196-200, 2016.
- [21] A. Salem, K. M. Rabie, K. A. Hamdi, E. Alsusa and A. M. Tonello, "Physical layer security of cooperative relaying power-line communication systems," *2International Symposium on Power Line Communications and its Applications (ISPLC)*, Bottrop, pp. 185-189, 2016.
- [22] A. Dubey, C. Kundu, T. M. N. Ngatched, O. A. Dobre and R. K. Mallik, "Incremental relaying for power line communications: performance analysis and power allocation," *IEEE Systems Journal*, vol. 13, no. 4, pp. 4236-4247, Dec. 2019.
- [23] M. Jani, P. Garg and A. Gupta, "Performance Analysis of a Mixed Cooperative PLC-VLC System for Indoor Communication Systems," *IEEE Syst. J.*, vol. 14, no. 1, pp. 469-476, March 2020.
- [24] I. S. Gradshteyn and I. M. Ryzhik, *Table of Integrals, Series, and Products*, 6th ed. New York: Academic Press, 2000.
- [25] P. V. Trinh, T. Cong Thang and A. T. Pham, "Mixed mmWave RF/FSO relaying systems over generalized fading channels with pointing errors," *IEEE Photonics Journal*, vol. 9, no. 1, pp. 1-14, Feb. 2017.
- [26] P. C. Sofotasios and S. Freear, "Novel expressions for the Marcum and one dimensional Q-functions," *7th International Symposium on Wireless Communication Systems (ISWCS)*, pp. 736-740, 2010.
- [27] L.-L. Yang and H.-H. Chen, "Error probability of digital communications using relay diversity over Nakagami-m fading channels," *IEEE Trans Wireless Commun.*, vol. 7, no. 5, pp. 1806-1811, May 2008.
- [28] The Wolfram functions site [Online]. Available: <http://functions.wolfram.com>.
- [29] L. Yang, F. Meng, J. Zhang, M. O. Hasna and M. D. Renzo, "On the performance of RIS-assisted dual-hop UAV communication systems," *IEEE Trans. Veh. Technol.*, vol. 69, no. 9, pp. 10385-10390, Sept. 2020.
- [30] I. S. Ansari, S. Al-Ahmadi, F. Yilmaz, M.S. Alouini, and H. Yanikomeroglu, "A new formula for the BER of binary modulations with dual-branch selection over generalized-K composite fading channels," *IEEE Trans. Commun.*, vol. 59, no. 10, pp. 2654-2658, Oct. 2011.
- [31] J. Park, E. Lee, G. Park, B. Roh and G. Yoon, "Performance analysis of asymmetric RF/FSO dual-hop relaying systems for UAV applications," *MILCOM 2013 - 2013 IEEE Military Communications Conference (MILCOM)*, pp. 1651-1656, 2013.